Multistability and Hysteresis in an Industrial Ammonia Reactor

E. Mancusi, G. Merola, and S. Crescitelli
Dipartimento di Ingegneria Chimica, Università Federico II, Piazzale Tecchio 80, I-80125 Napoli, Italy

P. L. Maffettone
Dipartimento di Scienza dei Materiali ed Ingegneria Chimica, Politecnico di Torino, I-10129 Torino, Italy

A model for an industrial ammonia reactor was studied with nonlinear-analysis tools. This model was recently considered to explain an industrial incident involving the onset of sustained oscillations due to a sudden decrease in the reactor pressure. The analysis was based on the bifurcation diagrams. Both multistability and hysteretic behaviors described here can be useful for an effective plant design, as well as for an adequate plant control and operation.

Introduction

In a recent article, Morud and Skogestad (1998) address the problem of an industrial incident in an ammonia production plant. The incident was caused by a sudden loss of stability induced by a decrease of reactor pressure. The instability caused the steady state to give way to a dynamic regime characterized by sustained oscillations. The reactor was operated without any control, since the plant was designed with the assumption that the Van Herden (1953) stability analysis was adequate. The problem is addressed with a local linear stability analysis that bypasses the limitations of the static analysis based on the Van Herden approach (Aris and Amundson, 1958; Stephens and Richards, 1973; Crescitelli, 1995; El Nashaie and Elshishini, 1996).

In Morud and Skogestad (1998), the analysis is performed on a nonlinear model consisting of two partial differential equations, and is capable of qualitatively interpreting the incident data. The onset of oscillations is correctly described in spite of the model simplicity, and, in order to reduce the risks of instability, a control strategy is proposed. One minor limitation of the approach of Morud and Skogestad (1998) is the lack of a complete dynamic analysis that, for example, prevents the possibility of disclosing other loss of stability scenarios that might be encountered in the actual operations.

In the present work, the results of a complete dynamic analysis (a complete and clear introduction on this subject can be found in Kutnezov (1998)) are presented. The same model proposed by Morud and Skogestad (1998) is considered to show how this approach can improve the model predicting capability. A thorough description of both static and dynamic attractors is made available for typical operating conditions. The reactor pressure (as in Morud and Skogestad, 1998) and the exchanger efficiency are considered as bifurcation parameters.

Model

Figure 1 shows the reactor that consists of three beds in series with fresh feed between each bed and preheating of the feed with the effluents. Both the heat exchanger and the mixers are considered to have no dynamics; the catalytic reactor is treated with a simple pseudo-homogeneous model with axial dispersion.

The model is written in terms of mass and energy balances, and is given by the following equations

$$0 = -w\frac{\partial c}{\partial z} - \rho_C r(T,c)$$

$$\rho_C C_{PC}\frac{\partial T}{\partial t} + w C_{PC}\frac{\partial T}{\partial z} = (-\Delta H_{rx})\rho_C r(T,c) + \Gamma\rho_C C_{PC}\frac{\partial^2 T}{\partial z^2} \tag{1}$$

In Eq. 1, the same notation of Morud and Skogestad has

Correspondence concerning this article should be addressed to S. Crescitelli.

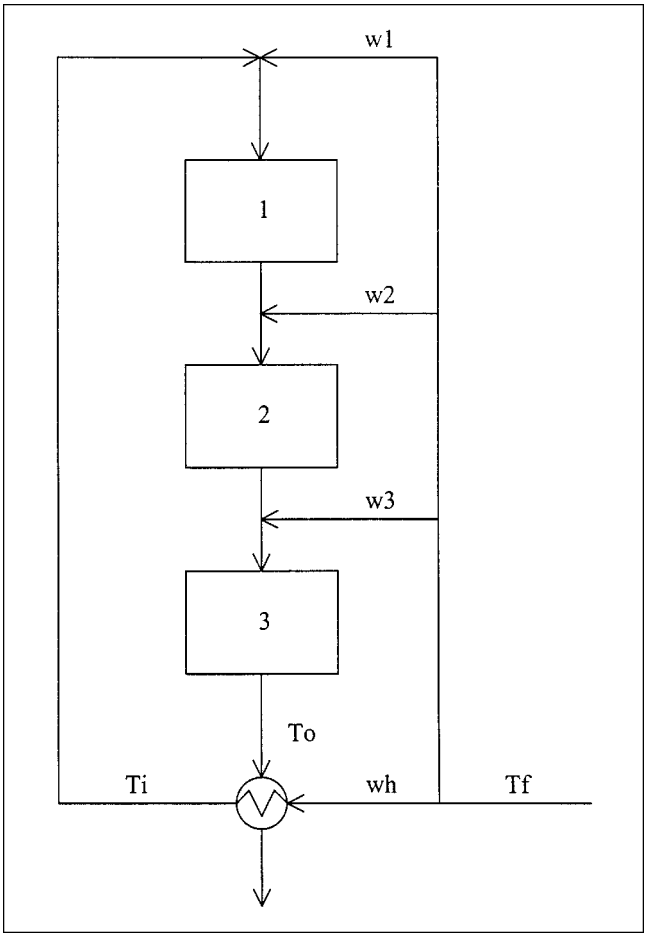

Figure 1. Ammonia reactor.

been adopted, and, as in Morud and Skogestad (1998), the gas-phase holdup is neglected. Indeed, we tested this assumption by accounting also for the gas holdup, and the predictions of Eq. 1 are always qualitatively and quantitatively very close to those predicted without the negligible-holdup assumption both for steady-state solutions and periodic ones.

The heat exchanger is modeled as a standard countercurrent exchanger without dynamics

$$T_i = \epsilon\, T_o + (1-\epsilon)\, T_f \tag{2}$$

where T_i is the exchanger outlet temperature, ϵ is the exchanger efficiency, T_o is the reactor outlet temperature, and T_f is the feed temperature.

The reaction kinetic for the reaction $N_2 + 3H_2 \leftrightarrow 2NH_3$ is Morud and Skogestad, 1998; Froment and Bischoff, 1990)

$$r_{N_2} = \frac{1}{\rho_{cat}}\left(k_1\, p_{N_2}\frac{p_{H_2}^{1.5}}{p_{NH_3}} - k_{-1}\frac{p_{NH_3}}{p_{H_2}^{1.5}}\right) \quad (\text{kmol } N_2/\text{kg}\cdot\text{cat, h}) \tag{3}$$

The model is studied with two different approaches: A continuation analysis is performed with the popular code AUTO97 (Doedel et al., 1997), and simulations are used to elucidate transients behaviors.

Both the numerical approaches are based on the same discretization scheme: a finite-difference, upwind scheme similar to that used by Morud and Skogestad (1998). In fact, to simplify the implementation in the continuation code, the model is considered without the negligible holdup assumption. A spatial discretization over 30 mesh-points is sufficient to accurately describe both the steady-state and the periodic solutions. As a consequence, upon discretization, the model is reduced to a set of 2×30 ordinary differential equations, which prove sufficient to correctly describe the model dynamics. The user-defined parts required by the continuation software are developed with Mathematica. By exploiting the symbolic capabilities of this software, we perform the automatic composition of the Fortran subroutines for AUTO. With this technique, the cumbersome algebra required to generate the righthand sides of the dynamic model, and the corresponding Jacobian matrix, is easily performed, so that the continuation of very large systems of ordinary differential equations (see, for example, Continillo et al., 2000), as in the present case, is easily made possible.

Results

All the results here reported have been calculated by using the same data reported in Morud and Skogestad (1998). The bifurcation study was conducted by considering as bifurcation parameters the reactor pressure P, and the exchanger efficiency ϵ. The continuation results are presented with two kinds of plots: the solution diagrams for P, and the bifurcation diagram in the plane $P-\epsilon$. The solution diagrams report, as a representation of the solution, either the temperature of the gas coming out of the reactor for the steady-state solutions, or, for limit cycles, the maximum outlet-temperature value attained during the oscillations. These quantities are plotted vs. the reactor pressure. On the other hand, the bifurcation diagram illustrates the loci of bifurcation points in the parameter space (Kubiçek and Marek, 1983). Some simulation results, for interesting operating situations, are also reported.

Figure 2 shows the solution diagram as the reactor pressure is varied ($\epsilon = 0.628$). In this figure (Figure 5), the solid lines represent stable stationary solutions, the dashed lines represent unstable stationary solutions, the filled circles represent stable periodic solutions, whereas the empty circles are unstable periodic solutions. Finally, filled squares represent Hopf bifurcation points. The pressure values at the bifurcation points are reported in Table 1. As first shown by Morud and Skogestad, the high conversion branch is stable from $P = 162.81$ bar. For this value of the pressure, a Hopf bifurcation (H1) is found, and the stationary stable solution becomes unstable as the pressure is decreased. This was the very same picture illustrated by Morud and Skogestad. Further decreasing the pressure, a limit point bifurcation (or saddle-node bifurcation) is first encountered (S1), then, another Hopf bifurcation (H2) is encountered along the unstable stationary branch. Finally, the stable low conversion branch is reached through another limit point bifurcation (S2). The continuation schemes allow for the determination of the dynamic branches departing from the Hopf bifurcations. The most im-

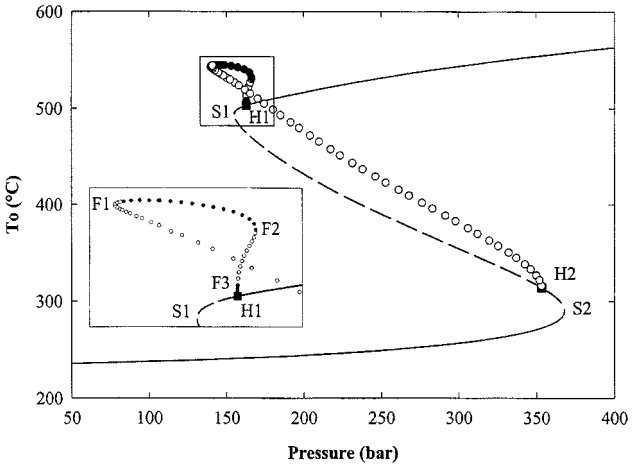

Figure 2. Solution for $\epsilon = 0.628$.

Solid lines: stable stationary solutions; dashed lines: unstable stationary solutions; filled circles; stable limit cycles; unfilled circles; unstable limit cycles; filled squares; Hopf bifurcations. The insert shows details of the delimited rectangular region.

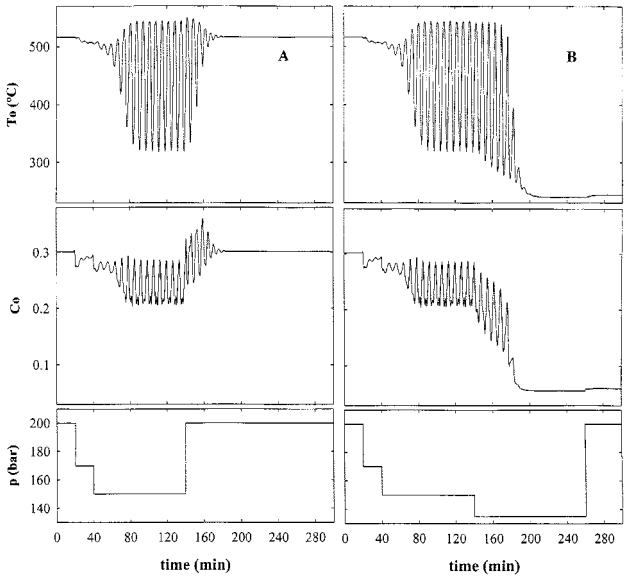

Figure 3. Possible loss of stability scenarios.

(A) Situation illustrated by Morud and Skogestad (1998); (B) Scenario revealed by the nonlinear analysis proposed in the present work.

portant feature of the model is the presence of the stable periodic solutions at high conversion (see the inset in Figure 2). The periodic regime emerges from the supercritical Hopf bifurcation (H1), and is initially stable. Then, after a limit point bifurcation on the periodic branch (or fold bifurcation) (F3), the periodic solution becomes unstable; a successive second fold bifurcation (F2) makes the solution stable again. It should be remarked that the presence of these two folds (F2 and F3) has a practical qualitative effect on the Hopf bifurcation (H1) that a local analysis is unable to describe. In fact, even though the Hopf bifurcation is supercritical, as can be demonstrated with a local analysis, from a practical point of view, it acts as a catastrophic subcritical one, since any ''small'' pressure reduction in the reactor larger than $|\Delta p| = |P_{H1} - P_{F3}| = 0.0014$ bar results in the jump from stable static solution to the stable periodic solution with large amplitude oscillations (the stable branch between F1 and F2). Finally, at $P = P_{F1}$, a fold (F1) marks the onset of the unstable branch that eventually dies on the second supercritical Hopf bifurcation (H2). The fold bifurcation (F1) plays an important role. In fact, a decrease in the reactor pressure from its steady-state set point is ''recoverable'' if P does not go below he left-most fold bifurcation value (P_{F1}). In that case the analysis of Morud and Skogestad is correct. If, on the other hand, the fold is surpassed ($P < P_{F1}$), then the model predicts the jump to the low conversion branch, and a successive increase of the reactor pressure could result in a new ''startup'' route along the low conversion branch up to the limit point at $P = P_{S2}$. Finally, note that the periodic solutions described here have a period of oscillation (not reported in the plot) always close to that experimentally measured and reported in Morud and Skogestad (1998) (420 s).

Table 1. Pressure values at the Bifurcation Points

$\epsilon = 0.628$		
	P (bar)	T_o (°C)
S1	155.1572	493.3967
S2	368.0220	290.3832
H1	162.8164	503.0905
H2	353.4878	313.9626
F1	139.7897	542.5780
F2	166.2252	507.8695
F3	152.8150	503.0954

Figure 3 reports the two possible loss of stability scenarios. Here, the uppermost plot shows the temperature evolution, the plot in the middle shows the concentration dynamics, and the lower most plot reports the pressure imposed policy. Figure 3A corresponds to the situation illustrated by Morud and Skogestad, whereas Figure 3B reports the new scenario here envisaged. It is apparent that, in the latter case, a decrease in the pressure determines the onset of oscillations that eventually die out, and the low conversion conditions are reached. It should be noted that, as reported in Figure 2, a multiplicity of stable attractors is also found. In details, a single low conversion static attractor is found for $P < P_{F1}$; for $P_{F1} < P < P_{F3}$, the static low conversion attractor and a periodic high conversion attractors are encountered; for $P_{F3} < P < P_{H1}$, two periodic stable limit cycles and one low conversion steady state are found; two static attractors and one stable limit cycle is predicted for $P_{H1} < P < P_{F2}$; two static attractors (again one with low conversions and the other with high conversions) are found in $P_{F2} < P < P_{S2}$; finally, only the stable stationary high conversion solution is found for $P > P_{S2}$.

Figure 4 shows the attractors for two different values of the reactor pressure: the solid lines give the spatial temperature profiles along the axial coordinate within the bed, and the dashed lines represent the periodic solutions with three profiles at three different times. Figure 4A (the two uppermost graphs) shows a case ($P = 164$ bar, $P_{H1} < P < P_{F2}$) when two stable stationary solutions are present together with a stable limit cycles. Figure 4B (the two lowermost graphs)

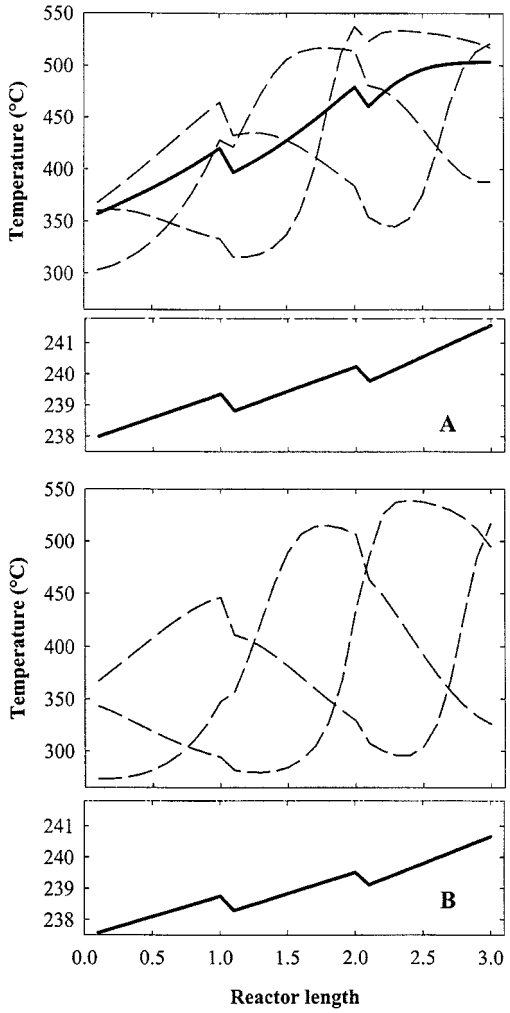

Figure 4. Attractors for two different situations.

(A) $P = 164$ bar (B) $P = 150$ bar. The temperature profile is along the reactor axial coordinate. The solid lines represent stable stationary solutions, and dashed lines represent the state of the reactor at three different times during the oscillation.

shows a case ($P = 150$ bar, $P_{F1} < P < P_{F3}$) when only the low conversion solution and a stable limit cycle are encountered. In both cases, during the periodic oscillation, the temperature overshoots the highest high-conversion stationary values.

The effect of the exchanger efficiency is illustrated in Figure 5, where the solution diagrams for $\epsilon = 0.350$ are reported. In this condition, four supercritical Hopf bifurcations are encountered, but only one stable limit cycle branch is found. The stable periodic branch emerges from the supercritical Hopf bifurcation (H1) and contains only one fold bifurcation F1. As for the case of Figure 3, the pressure P_{F2} marks the limit of high conversion operability. It should be remarked that the two folds, F2 and F3, that are present in Figure 2, have disappeared since they coalesced for $\epsilon = 0.54$ and $P = 200$ bar; it can be noted, in fact, that the shape of the stable periodic branch emerging from the Hopf bifurcation (H1) is reminiscent of the coalescence.

A better insight can be obtained by considering the bifurcation diagram in the plane $P - \epsilon$ reported in Figure 6. The

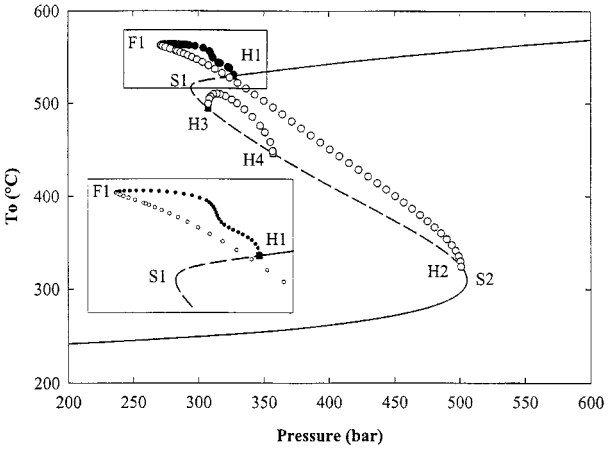

Figure 5. Solution for $\epsilon = 0.35$.

Solid lines: stable stationary solutions; dashed lines: unstable stationary solutions; filled circles; stable limit cycles; unfilled circles: unstable limit cycles; filled squares: Hopf bifurcations. The inset shows details of the delimited rectangular region.

lines reported in this plot divide the parameter space in regions characterized by qualitatively similar phase portraits: solid lines represent Hopf bifurcations, dashed lines represent limit point bifurcations, and double-dot-dashed lines represents the fold bifurcation lines. The lowermost diagram represents the real situation, whereas, in the uppermost diagram, the scales have been deliberately altered for the sake of clarity. In this part of the figure, the number and the type of steady state and dynamic solutions are also reported. Four numbers identify a region: the left ones give the number of steady-state solutions (the upper one) and of the limit cycle solutions (the lower one), while on the right (in square brackets) the corresponding number of stable solutions is reported. It should be remarked that the Hopf bifurcation line corresponding to the bifurcations like H_3 and H_4 of Figure 5 is a closed curve. On the other hand, the bifurcations like H1 and H2 (in Figures 2 and 3) also lie on a unique bifurcation line. Note that, for $P > 848.2$ bar, and for $\epsilon < 0.013$, no Hopf bifurcation is encountered, and there is no stable limit cycle. The "important" fold bifurcation, that is, the one that marks the limits of high conversion stable limit cycles (F1 in Figure 3e and in Figure 4) is the rightmost fold bifurcation line. The other two fold bifurcation lines merges onto the Hopf bifurcation line for $P = 200$ bar and $\epsilon = 0.54$.

Finally, note that many higher-codimension bifurcations (Kuznetsov, 1998) are present (cusps in the bifurcation lines and crossing of bifurcation lines).

Conclusions

The complete dynamical study of the model proposed by Morud and Skogestad (1998) to describe the ammonia production reactor has been presented. The analysis has been performed with a continuation code properly interfaced with a symbolic software. As recently highlighted also by Seider et al. (1999), the complete dynamical characterization of a model is very useful to study multistability and its influence on plant design, control, and operation.

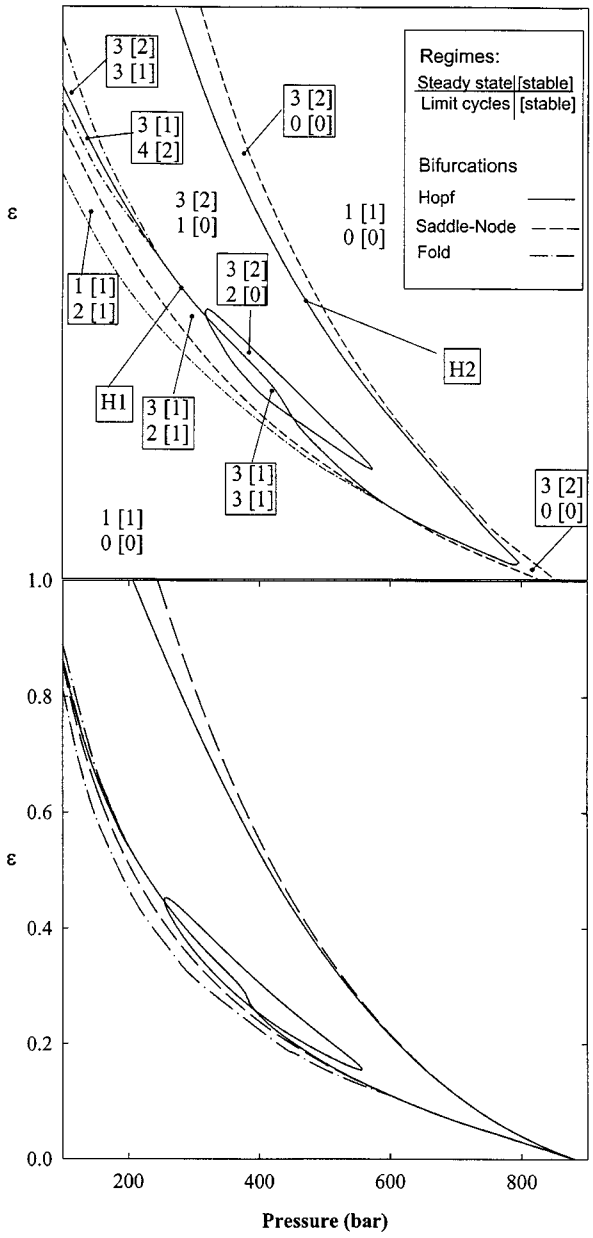

Figure 6. Bifurcation in the plane $P-\epsilon$.

(A) Bifurcation lines are in the real scales; (B) the lines are distorted for the sake of clarity. The inset shows the number of stationary and periodic solution and their stability properties pertaining to each region.

For the problem at hand, complex hysteretic phenomena and multistability have been found and characterized. Indeed, the presence of fold catastrophic bifurcations on periodic solution branches requires a careful control strategy to avoid the process shut-off. Thus, the knowledge of the global dynamics can be helpful in designing an effective control strategy. In the near future, we will address this problem by considering the global control approach (Shahrestani and Hill, 1998) as a possible candidate for processes with a dynamics similar to that reported in the present work.

Acknowledgments

This research was partly funded by Gruppo Grandi Rischi (CNR) and by MPI MURST.

Notation

c = ammonia mass fraction
C_{PC} = catalyst specific heat
C_{PG} = gas specific heat
k_1, $k-1$ = direct and inverse rate constants
m_C = catalyst mass in the bed
p_i = partial pressure of component i
r = reaction rate
t = time
T = temperature, K
w = gas mass flux
z = reactor axial coordinate
Γ = dispersion coefficient
ΔH = heat of reaction
ρ_{cat} = catalyst density

Literature Cited

Aris, R., and N. R. Amundson, "An Analysis of Chemical Reactor Stability and Control," *Chem. Eng. Sci.*, **7**, 121 (1958).
Doedel, E. J., A. R. Champneys, T. F. Fairgrieve, Y. A. Kuznetsov, B. Sanstede, and X. Wang, *AUTO97: Continuation and Bifurcation Software for Ordinary Differential Equations* (July 1997).
Continillo, G., V. Faraoni, P. L. Maffettone, and S. Crescitelli, "Non-linear Dynamics of a Self-Igniting Reaction-Diffusion System," *Chem. Eng. Sci.*, **55**, 303 (2000).
Crescitelli, S., "Nonlinear Analysis and Dynamic Behavior of Chemical Reactors," *Analysis, Stability and Dynamics of Chemical Reactors*, G. Continillo, S. Crescitelli, and P. G. Lignola, eds., Cuen, Napoli (1995).
Froment, G. F., and K. B. Bischoff, "Chemical Reactor Analysis and Design, 2nd ed., Wiley, New York (1990).
El Nashaie, S. S. E. K., and S. S. Elshishini, *Dynamical Modelling, Bifurcation and Chaotic Behaviour of Gas-Solid Catalytic Reactors*, Gordon and Breach, Amsterdam (1996).
Kuznetsov, Y. A., Elements of Applied Bifurcation Theory, 2nd ed., Springer Verlag, New York (1998).
Kubiçek, M., and M. Marek, *Computational Methods in Bifurcation Theory and Dissipative Structure*, Springer Verlag, New York (1983).
Morud, J. C., and S. Skogestad, "Analysis of Instability in an Industrial Ammonia Reactor," *AIChE J.*, **44**, 888 (1998).
Seider, W. D., T. D. Seader, and D. R. Lewin, *Process Design Principles: Synthesis, Analysis and Evaluation*, Wiley, New York (1999).
Shahrestani, S. S., and D. J. Hill, "Global Nonlinear Control with Applications to Power Systems," *Proc. Eur. Control Conf. Bruxelles*, (June, 1998).
Stephens, A. D., and R. J. Richards, "Steady State and Dynamic Analysis of an Ammonia Synthesis Plant," *Automatica*, **9**, 65 (1973).
Van Herden, C., "Autothermic Processes. Properties and Reactor Design," *Ind. Eng. Chem.*, **45**, 1242 (1953).

Manuscript received June 29, 1999, and revision received Oct. 27, 1999.